Anat Embryol (1992) 186:167–173

Anatomy and Embryology
© Springer-Verlag 1992

Silver impregnability of ischemia-sensitive neocortical neurons after 15 minutes of cardiac arrest in the dog

Ivo Vanický, Martin Maršala, Judita Orendáčová, and Jozef Maršala

Institute of Neurobiology, Slovak Academy of Sciences, Šrobárova 57, 040 01 Košice, Czechoslovakia

Accepted February 17, 1992

Summary. The development of postischemic neuronal argyrophilia and the subsequent fate of argyrophilic neurons were studied in dogs after 15 min of complete cerebral ischemia and survival varying from 1 h to 7 days. Histopathological examination of the vulnerable neocortical region was performed using the Nauta degeneration method, and the time course of cellular changes was described. Clear-cut neuronal argyrophilia was found to precede cell body shrinkage and gradual disintegration corresponding to selective neuronal death. To clarify this initial stage of neuronal impregnability, the samples from the animals surviving 8 h postarrest were stained with toluidine blue or processed for electron microscopy, and the distribution of argyrophilic cells was confirmed to be identical with that of hyperchromatic or electron-dense cells. On the other hand, infrequently observed "tissue infarctions" exhibited no silver affinity in spite of apparent cellular damage. These findings indicate that enhanced impregnability is related to cytochemical processes incidental to the phenomenon of "selective neuronal death", which can be readily detected by the Nauta method.

Key words: Argyrophilia – Cardiac arrest – Dog – Ischemia – Somatosensory cortex

Introduction

A typical form of ischemia-induced neuronal injury is represented by the occurrence of "dark" or "ischemic" neurons, (Pulsinelli et al. 1982; Jenkins et al. 1981; Smith et al. 1984; Blomqvist and Wieloch 1985). They appear in the vulnerable cerebral regions after different postischemia "maturation" periods, and their visualization by routine histological staining is rather difficult. Moreover, dark neurons are gradually eliminated from the tissue (Auer et al. 1984; Nedergaard 1988), and therefore only reduced cell numbers can be found after longer survival periods. Recently, silver degeneration methods, originally developed for tracing axonal and terminal degenerations, have been found extremely useful for visualizing neuronal changes after transient CNS ischemia (Crain et al. 1988; Maršala et al. 1989; Gallyas et al. 1990). Enhanced somato-dendritic impregnability was presumed to correspond to "dark" neurons (Crain et al. 1988; Gallyas et al. 1990) which usually show other typical pathomorphological changes, such as shrunken outlines, pyknotic nuclei and corkscrew like dendrites. In the Nauta impregnated sections, we have repeatedly observed argyrophilic Golgi-like neurons without signs of other changes. This picture was typical for early recirculation periods, and it stimulated us to investigate whether enhanced somatodendritic argyrophilia precedes alterations otherwise detectable by standard histological techniques. We have used both toluidine blue staining and electron microscopy to compare consecutive sections from the tissue containing argyrophilic Golgi-like neurons. The somatosensory cortex was chosen for a detailed cellular study because this area shows extensive degeneration of relatively homogeneous neuronal populations, and their postischemic "maturation" is rather slow (Lin et al. 1990).

Correspondence to: I. Vanický

Material and methods

A modified canine model of 15-min cardiac arrest (Kumar et al. 1987) was used. Twenty eight adult mongrel dogs weighing 14–22 kg fasted 24 h before intervention, with free access to water. After pentobarbital anesthesia (30 mg/kg i.v.), the animals were intubated and artificially ventilated with the volume ventilator (Anemat N8, CSFR) using room air. The tidal volume of 15 ml/kg and respiratory rate were adjusted to assure physiological levels of arterial blood gases (pO_2 between 90 and 110 Torr, pCO_2 between 30 and 40 Torr). The femoral vein and artery were cannulated for fluid and drug administration and for monitoring of mean arterial blood pressure (MABP), respectively. A silicon catheter was introduced into the right atrium for KCl administration via the left external jugular vein. Two-channel bilateral EEG was recorded using silver electrodes glued to the skull. MABP, EEG

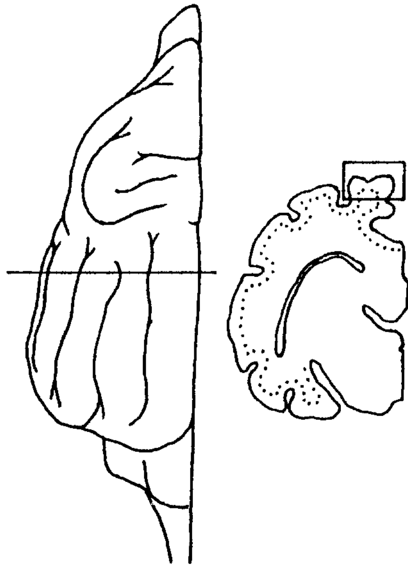

Fig. 1. A hemisphere and transverse section specifying the site from which samples were obtained

and ECG were continuously monitored during intervention. A left side thoracotomy was performed in the fifth intercostal space for open chest cardiac massage (OCCM) and internal defibrillation. The pericardium was not opened. Cardiac arrest was then induced by injection of 0.75 mEq KCl/kg via the central vein catheter, and ventilation was turned off. Complete cardiac arrest was confirmed by immediate pulselessness, drop in MABP and loss of ECG activity. EEG activity became isoelectric within 30 s. The animals were kept in complete circulatory arrest (no flow) for 15 min. Resuscitation was then started with OCCM and ventilation with 100% oxygen. A bolus of epinephrine (0.1 mg/kg) and $NaHCO_3$ infusion (10 mEq/kg) with heparin (150 U/kg) were administered at the onset of resuscitation. In the 5th min of OCCM (MABP > 80 Torr) the heart was defibrillated (repeated if necessary). All animals restored spontaneous heartbeat after 5–9 min of resuscitation. Post-resuscitation tachycardia was controlled by 1% mesocain. MABP was maintained above 100 Torr with low dose epinephrine infusion (0.5 mg/200 ml of saline). After stabilization of cardiac activity and arterial pressure the chest was closed. Arterial blood gases and acid-base changes were periodically controlled (AVL-995Hb, Austria) and maintained within physiological ranges. All animals restored spontaneous breathing within 6–12 h after resuscitation. Body temperature was measured by an esophageal thermistor probe and maintained at $37.5 \pm 1°$ C using heating pad and lamps. The routine intensive care lasted for 12 h. All animals were regularly given antibiotics (Penstrepten) postoperatively. Long-term surviving animals exhibited severe neurological deficit. If they survived more than 24 h, most of them had to be given food and drink by an esophageal tube. Care was taken to minimize suffering of the animals during the whole experimental period, and occasional excitations during the postcomatose period were alleviated with diazepam. Animals survived 1 h ($n=5$), 8 h ($n=6$), 24 h ($n=4$), 3 days ($n=6$) and 7 days ($n=3$). In addition, four animals undergoing the same surgical procedures without circulatory arrest served as controls.

After their survival period, all animals were heparinized (200 U/kg), deeply anesthetized with pentobarbital (50 mg/kg i.v.) and transcardially perfused with saline (1-min flush) followed by 10% neutral formol (0.5 l/kg). Both solutions were prewarmed to 37° C and infused at a pressure of 130 mm Hg. The brain was removed 24 h later and immersed in the same fixative for 14 days. Blocks 5 mm long were dissected bilaterally from the suprasplenial gyrus (Fig. 1) and frozen sections cut at 20 μm were impregnated by the Nauta method (Nauta 1957). Four animals, (two controls, two 8 h post arrest survival), were fixed by transcardiac perfusion of 4% paraformaldehyde in 0.1 M phosphate buffer (pH = 7.4). For comparison, two blocks of the suprasplenial gyrus were dissected and processed separately either for electron microscopy or for the Nauta method. For electron microscopy the tissue was postfixed in 1% buffered OsO_4; semi-thin sections were stained with toluidine blue and ultrathin sections were stained with uranyl acetate followed by lead citrate. We avoided using glutaraldehyde because of non-specific mitochondrial costaining in silver impregnated sections (Gallyas et al. 1980). All precautions for the fixation process and handling of the material (Cammermeyer 1978) were observed to eliminate artificial brain traumatization.

Results

Time course of neuronal changes visualized by the Nauta method

Control animals

No increased argyrophilia can be found in control sections, and cell bodies as well as neuropil are lightly and uniformly stained. Neuronal perikarya are transparent with indistinct cell body outlines, and only the prominent nuclei indicate the identity and position of the cell bodies (Fig. 2a).

Post arrest survival for 1 h. Most neurons appear normal, although some of them contain fine silver deposits in the cytoplasm. Solitary neurons with enhanced somatodendritic argyrophilia can be found in the third layer (Fig. 2b).

Survival for 8 h. Most neurons in the second and third layers are heavily impregnated, as well as solitary ones in the fifth and sixth layers. This typical distribution has been noted in four of six animals; two dogs exhibited only occasional argyrophilic neurons in the vulnerable layers. The Golgi-like argyrophilia involves neurons completely, including their fine dendritic ramifications. A small number of affected neurons exhibits only heavily impregnated nuclei with perikarya remaining either transparent or displaying various degrees of impregnability. Many of the argyrophilic neurons exhibit no alterations of their soma outlines except for a corkscrew like appearance of their dendrites (Fig. 2c).

Survival for 24 h. The typical pattern of somatosensory cortical damage is fully developed. Neurons of various types and sizes are argyrophilic, but their dendritic ramifications are unclear and show irregular impregnation (Fig. 2d).

Survival for 3 days. The dendritic ramifications are almost completely undetectable but the cell bodies still persist in their typical laminar distribution. Moreover, numerous silver granules can be observed in the neuropil (Fig. 2e).

Survival for 7 days. The damaged neurons have mostly disappeared, although some of them still persist as poorly identifiable dark patches. In some places long apical dendrites can be traced as indistinct drop-like silver deposits (Fig. 2f).

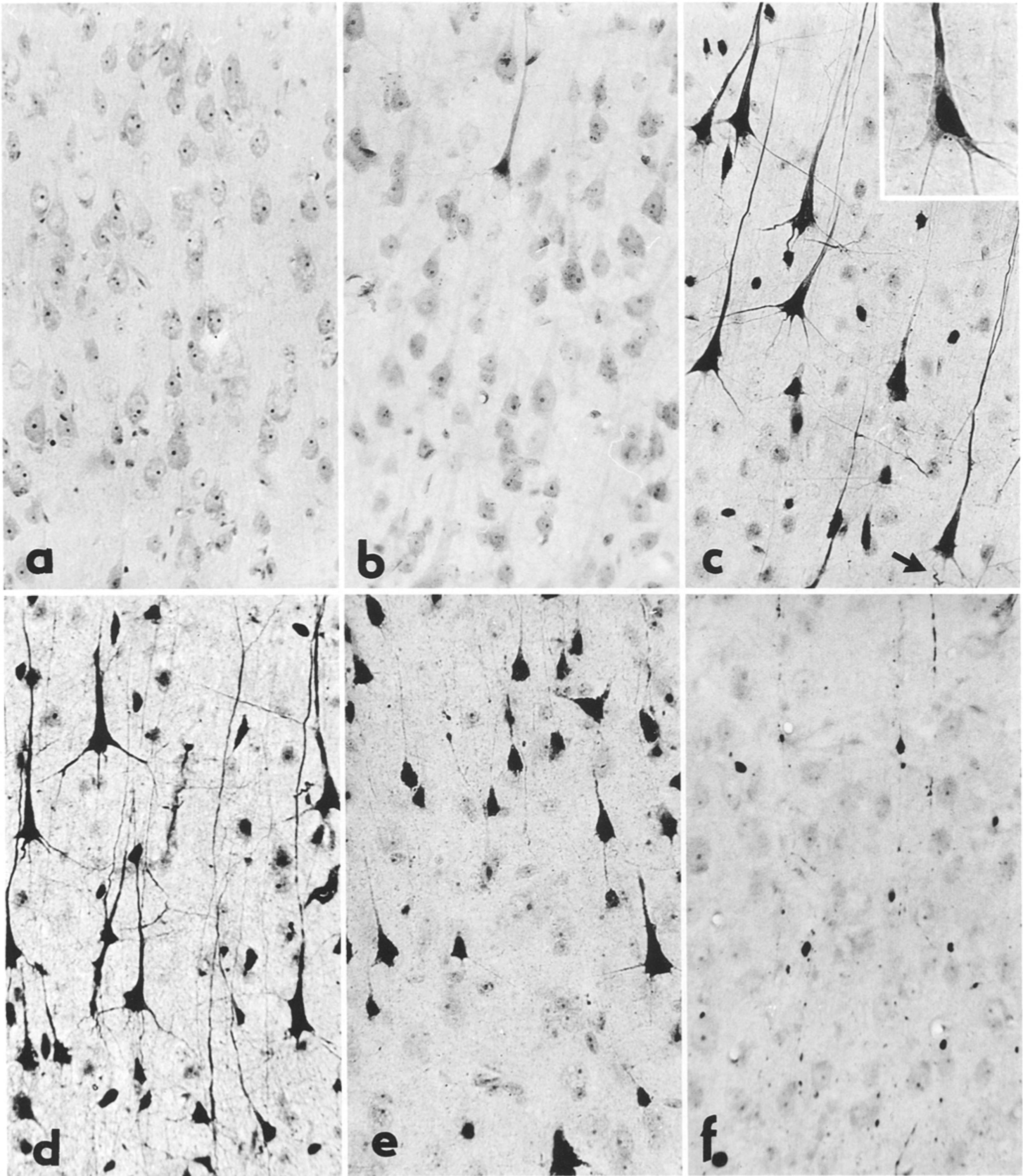

Fig. 2a–f. Development of cellular changes in the third neocortical layer visualized by the Nauta method. **a** Control. Poor visualization of cellular morphology (×175) **b** Survival for 1 h. A solitary impregnated neuron (×175) **c** Survival for 8 h. Golgi-like neuronal argyrophilia; a corkscrew-like dendrite can be seen (*arrow*); detail shows a neuron with dark nucleus and slightly impregnated perikaryon/dendrites (×175; *inset* ×260) **d** Survival for 24 h. Argyrophilic cells show deformities and irregular impregnation of dendritic processes (×175) **e** Survival for 3 days. Persisting argyrophilic cell bodies, but their processes have mostly disappeared (×175) **f** Survival for 7 days. Small patches and rows of silver deposits indicate remnants of cells and their processes (×175)

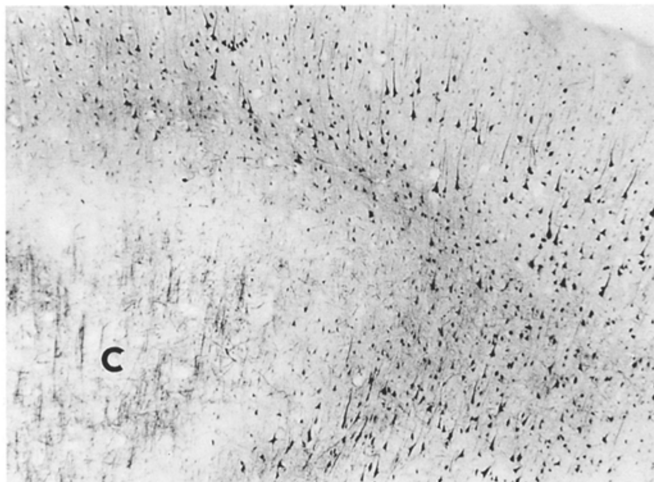

Fig. 3. Cortical infarction in a dog surviving 8 h. Note unclear structure of central infarction zone (*C*), pale border and many impregnated neurons surrounding it (Nauta impregnation, ×80)

Brain tissue infarctions. In four of the experimental dogs, small infarction foci were observed in the examined area. They were present in the animals surviving 8 h and longer and they seemed unpredictable with regard to their localization. No selective cellular impregnability was found in their central zone in spite of apparent cellular damage, irrespective of survival period. In the periphery, the infarction site was surrounded by many impregnated neurons (Fig. 3).

Nauta somatodendritic impregnability compared with toluidine blue staining and ultrastructural alterations

Control animals

Nauta impregnation. No increased argyrophilia can be observed in the control animals fixed with paraformaldehyde, and the picture is identical with that of control animals described above.

Toluidine blue. Semi-thin sections stained with toluidine blue show similar stainability of cellular perikarya and neuropil, therefore the cell shapes are difficult to recognize.

Electron microscopy. Ultrastructurally, neuronal perikarya exhibit normally distributed and well preserved organelles. The nuclei contain dispersed chromatin and well preserved nucleoli.

Survival post arrest for 8 h

Nauta impregnation. The fixative did not influence the typical neuronal impregnability, and the characteristic distribution of argyrophilic neurons described in formol-fixed animals was confirmed in the tissue adjacent to the samples processed for electron microscopy.

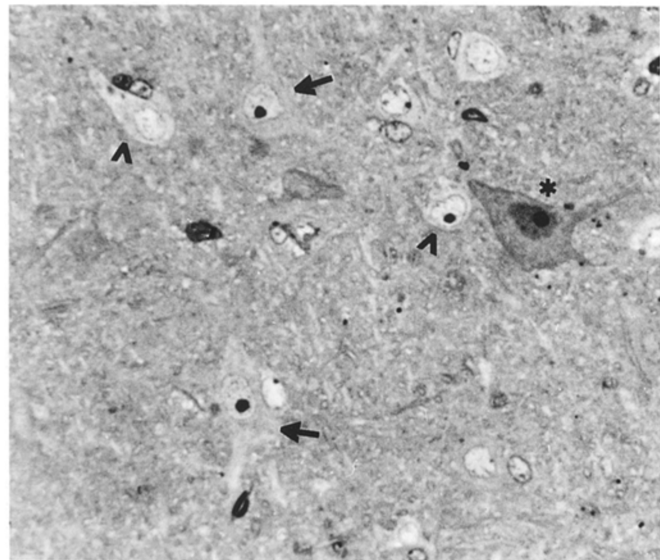

Fig. 4. Two basic types of neuronal response to ischemia after 8 h survival. Normal-appearing cells (*arrows*) and pale neurons (*arrowheads*) as well as a slightly darker one (*asterisk*) are visible. (Toluidine blue, ×516)

Toluidine blue. Numerous hyperchromatic cells were found distributed in a similar way to the argyrophilic ones described above. This neuronal change varied from slight hyperchromatosis to intensive staining and cell pyknosis. In slightly darkened neurons, the nuclei are always darker than the perikarya. This fact was used as a criterion for classifying them as "dark" neurons, since their cell bodies often seemed unaltered otherwise, and perikaryal darkening was absent in many of them (Fig. 4). In addition, many neurons became pale against the neuropil background, and this stage, easily detected by toluidine blue, was not apparent in the silver impregnated sections.

Fig. 5a–f. Ultrastructure of neuronal changes in the dog surviving 8 h post arrest. All neurons are from the third layer. Overall views on electron-lucent (**a**, **c**) and electron-dense (**b**, **d**) neurons; ×4,800. *Insets*: adjacent semi-thin sections stained with toluidine blue; ×260. **a** Electron-lucent neuron exhibiting only distinct cellular abnormalities. Note similar electron density of nucleus (*N*), perikaryon and neuropil. **b** Electron-dense neuron with unaltered outlines. Note darkened karyo- and cytoplasm as compared to neuropil. Dispersed nuclear chromatin and cytoplasmic vacuolization are apparent. Neighboring astrocytes (*A*) are almost unaltered (*right*) or show moderate swelling (*left*). **c** Pale neuron. Diffuse pallor is caused by perikaryal swelling; nucleus (*N*) contains clumped chromatin and condensed nucleolus. **d** Markedly shrunken homogeneously dark neuron. Neighboring astrocyte (*A*) is extremely swollen. Details from the pale (**e**) and electron-dense (**f**) neurons respectively; ×10,300: **e** Detail from **c**; cisterns of endoplasmic reticulum are shortened and some of them dilated (*arrows*). Both attached and free polyribosomes are dispersed. Swollen mitochondria with cristae disruption can be seen. **f** Detail from **b**. Cyto- and karyoplasmic matrix are darkened. In the cytoplasm, dispersed ribosomes and numerous groups of small vacuoles can be seen. Undamaged as well as swollen mitochondria are present

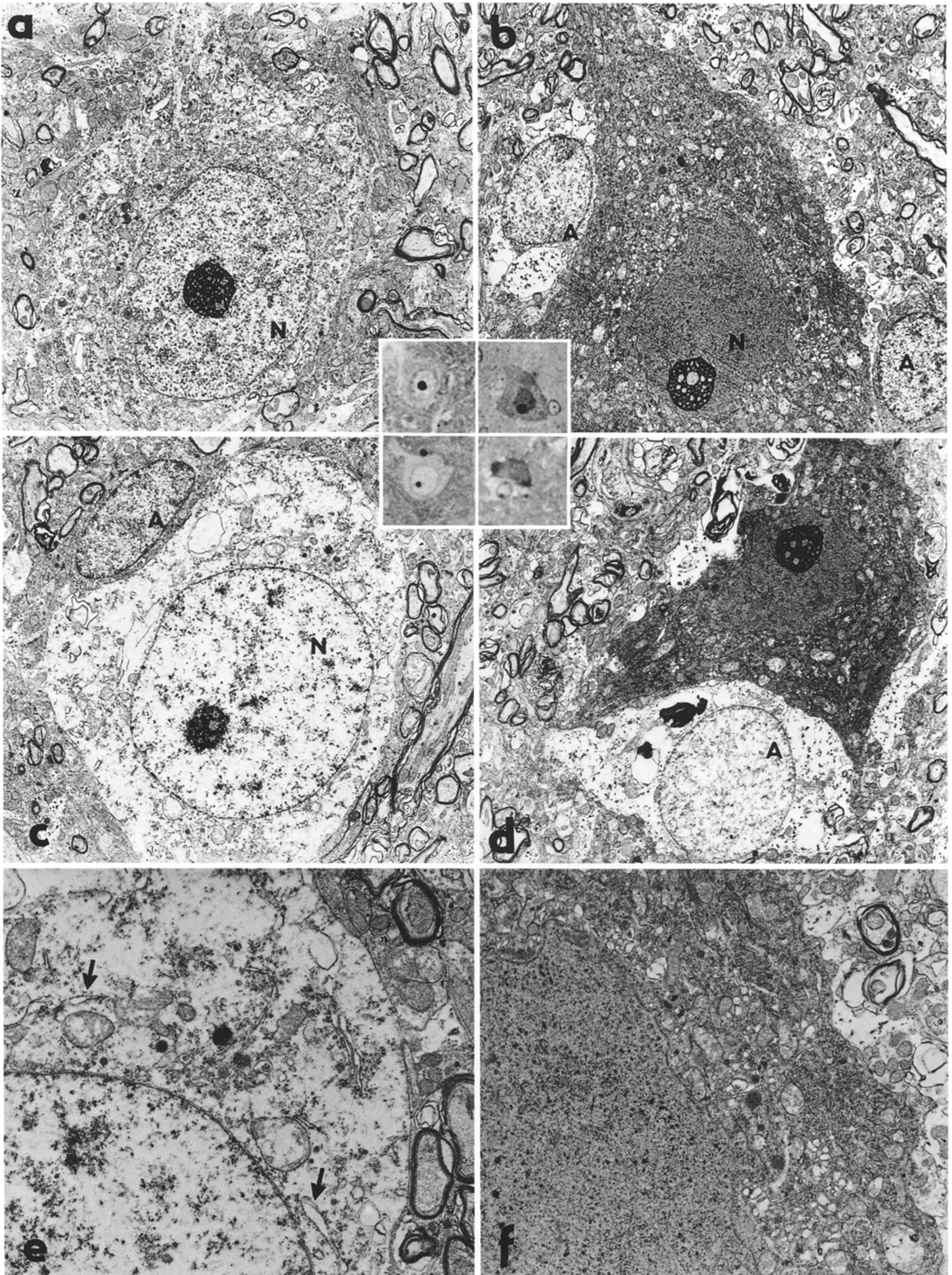

Fig. 5a–f

Electron microscopy. Two basic types of cellular response were found:

1. Neurons with electron-lucent cytoplasm. Most of these show only mild alterations, consisting of more or less pronounced nuclear chromatin clumping and nucleolar condensation. Within the cytoplasm, polyribosomes are decreased or absent, and the number and length of rough endoplasmic reticulum cisterns are reduced. The Golgi apparatus consists of vesicles rather than the usual cisterns. Most mitochondria are of normal appearance but some of them show swelling and abnormalities or even loss of mitochondrial matrix. In semithin sections, these neurons exhibit normal staining (Fig. 5a). Moreover, neurons with diffusely decreased electron density are present mainly in the third layer. Their nucleolus is condensed and degranulated, and the chromatin clumping is expressive. The ribosomes seem reduced in number, but some polyribosomes can be found. Large vacuoles are visible probably representing dilated Golgi cisterns and swollen mitochondria. The cell body as such exhibits moderate swelling, corresponding with diffuse pallor detected in semithin sections (Fig. 5c).
2. Neurons with increased electron density, characterized by a great variation of changes. Most of them exhibit unaltered soma size or shape and only a moderately increased electron density of their cytoplasm and karyoplasm. In the nucleus, usually a well preserved nucleolus and dispersed chromatin are found. Within the neuronal cytoplasm, only more or less advanced structural alterations, similar to those described in the electron lucent neurons, are observed. In addition, their cytoplasm contains numerous irregularly dispersed vacuoles, and ribosomes are present only as monoribosomes. This corresponds with slight neuronal hyperchromatosis observed in semithin sections (Fig. 5b).

In extremely electron-dense cells, which are usually shrunken, the intracellular organelles are almost indistinguishable. The cell body shrinkage is always accompanied by astrocytic swelling and enlargement of glial processes. In semithin sections, these neurons correspond with hyperchromatic and shrunken cells (Fig. 5d). In general, the electron-dense neurons display various intermediate forms between the two extreme types described above.

Discussion

The Nauta degeneration method used in our study represents a useful technique for visualizing the development of ischemia-induced neuronal damage. Somato-dendritic argyrophilia, as a response to neuronal injury, was first described after hypoglossal nerve transection in young kittens (Grant and Aldskogius 1967). More recently, silver degenerating methods were used in various experiments by others (Switzer 1976; Heimer and Kalil 1978; Crain et al. 1988; Maršala et al. 1989; Lin et al. 1990; Sloviter 1991). In recent studies on ischemic CNS injury, selective neuronal argyrophilia was presumed to be related to an electron-dense form of degeneration (Crain et al. 1988; Gallyas et al. 1990), but no attempts were made to clarify the mechanisms accounting for the increased silver affinity. This "dark" form of cellular response, originally denoted as ischemic cell change (Brown and Brierley 1971) has been described under numerous synonyms, such as hyperchromatic, shrunken and homogeneous or acidophilic neurons etc. "Dark" neurons were observed after various pathological insults including hypoglycemia (Auer et al. 1984), status epilepticus (Ingvar et al. 1988), trauma (Van den Pol and Gallyas 1990) and neurotoxic agents (Gallyas et al. 1990). In general, "dark" neurons were described as shrunken or pyknotic, and increased cellular density was presumed to be in direct relation to cellular shrinkage (Jenkins et al. 1981). On the other hand, argyrophilia seems to develop abruptly in an otherwise well-preserved neuron, and it probably reflects a certain cytochemical change affecting the whole cell body. Comparison with toluidine blue staining indicates that early argyrophilia corresponds with slight hyperchromatosis. Our electron microscopical analysis was carried out to determine the ultrastructural correlate to the increased stainability of these non-shrunken hyperchromatic neurons. Ultrastructurally, all these neurons exhibit a darkened nuclear and cytoplasmic matrix. The cytoplasmic organelles however show highly variable changes. It is therefore tempting to attribute the selective neuronal argyrophilia to some biochemical/biophysical alteration of the cytoplasm and cytoskeleton in response to ischemia-reperfusion-induced injury.

The biochemical basis of this phenomenon remains unclear. Although various neuronal alterations have been described in early recirculation periods or even after ischemia alone (Jenkins et al. 1981; Seubert et al. 1989; Yanagihara et al. 1990), none of them exhibit such a clear correlation with irreversible neuronal damage as argyrophilia. The events immediately preceding morphologically detected neuronal damage are of special importance, since they might explain the selectivity of neuronal response to ischemia. Recent immunohistochemical studies have provided evidence about the induction of so called heat shock proteins shortly after ischemia. The dynamics and distribution of their immunoreactivity are closely related to, but not completely identical with, selective neuronal damage (Gonzalez et al. 1991; Sharp et al. 1991). However, their increasing synthesis in the injured cells has been considered to act as a protective rather than detrimental factor. The heat shock proteins therefore seem to play only a part in the early cell response to injury (Sharp et al. 1991). Recently, an excellent correlation of neuronal injury with tissue levels of polyamine metabolites (especially putrescine) has been reported after various pathological insults including ischemia (Paschen et al. 1987). Putrescine has been shown to contribute to calcium-related membrane activities, but its role in the chain of pathophysiological events causing neuronal necrosis is not exactly determined (Paschen et al. 1991). Neuronal death is known to be coupled with accumulation of calcium which triggers numerous proteolytic enzymes (Siesjö 1988), and the intracellular calcium loading probably closely correlates with neuronal argyrophilia. In relation to ischemic pathophysiology, the onset of argyrophilia might reflect the stage when

membrane functions fail and subsequent alterations of structural molecules come into play. These alterations, however, seem to be conditioned by other specific factors since the electron dense form is not a ubiquitous sign of cellular damage. Simultaneously with the "dark" form, we have observed pale neurons, which probably correspond to the early diffuse pallor described in gerbils (Nishikawa et al. 1989); this cellular change is probably transient. Curiously, no argyrophilia was detected in the central infarction zone. Our observations, confirmed also in other cerebral regions, are in accordance with those described after permanent occlusion of the middle cerebral artery (Nedergaard 1988) and after cerebral ischemia in hyperglycemic rats which develop multiple infarctions rather than selective neuronal death (Kalimo et al. 1981). However, the presence of argyrophilic cells in the border of the infarct indicates the role of the recirculation phase in "dark" neuronal transformation (Jenkins et al. 1981). Some other general mechanisms involved in the development of "dark" neuronal response are indirectly indicated by their occurrence after experimental hyperstimulation (Agnew et al. 1983; Clarke and Nussbaumer 1987) and excessive tissue acidosis (Kraig et al. 1987), but the biochemical substrates responsible for the increased cellular argyrophilia remain to be elucidated. Our ultrastructural findings draw attention to the changes of karyo- and cytoplasmic basal matrix which seem to coincide with the onset of neuronal argyrophilia.

References

Agnew WF, Yuen TGH, McCreery DB (1983) Morphologic changes after prolonged electrical stimulation of the cat's cortex at defined charge densities. Exp Neurol 79:397–411

Auer RN, Wieloch T, Olsson Y, Siesjö BK (1984) The distribution of hypoglycemic brain damage. Acta Neuropathol (Berl) 64:177–191

Blomqvist P, Wieloch T (1985) Ischemic brain damage in rats following cardiac arrest using a long-term recovery model. J Cereb Blood Flow Metab 5:420–431

Brown AW, Brierley JB (1971) The nature and time course of anoxic-ischemic cell change in the rat brain. An optical and electron microscope study. Clin Dev Med 39/40:49–60

Cammermeyer J (1978) Is the solitary dark neuron a manifestation of post mortem trauma to the brain inadequately fixed by perfusion? Histochemistry 56:97–115

Clarke PGH, Nussbaumer JC (1987) A stain for ischaemic or excessively stimulated neurons. Neuroscience 23:966–979

Crain BJ, Westerkam WD, Harrison AH, Nadler JV (1988) Selective neuronal death after transient forebrain ischemia in the mongolian gerbil: a silver impregnation study. Neuroscience 27:387–402

Gallyas F, Wolff JR, Bottcher H, Zaborszky L (1980) A reliable and sensitive method to localize degeneration and lyzozomes in the central nervous system. Stain Technol 55:299–306

Gallyas F, Guldner FH, Zoltay G, Wolff JR (1990) Golgi-like demonstration of "dark" neurons with an argyrophil III. method for experimental neuropathology. Acta Neuropathol (Berl) 79:620–628

Gonzalez MF, Lowenstein D, Fernyak S, Hisanaga K, Simon R, Sharp FR (1991) Induction of heat shock protein 72-like immunoreactivity in the hippocampal formation following transient global ischemia. Brain Res Bull 26:241–250

Grant G, Aldskogius H (1967) Silver impregnation of degenerating dendrites, cells and axons central to axonal transection. I. A Nauta study on the hypoglossal nerve of kittens. Exp Brain Res 3:150–162

Heimer L, Kalil R (1978) Rapid transneuronal degeneration and death of cortical neurons following removal of the olfactory bulb. J Comp Neurol 178:559–610

Ingvar M, Morgan PF, Auer RN (1988) The nature and timing of excitototoxic neuronal necrosis in the cerebral cortex, hippocampus and thalamus due to fluorothyl-induced status epilepticus. Acta Neuropathol (Berl) 75:362–369

Jenkins LW, Povlishock JT, Lewelt W, Miller JD, Becker DP (1981) The role of postischemic recirculation in the development of ischemic neuronal injury following complete cerebral ischemia. Acta Neuropathol (Berl) 55:205–220

Kalimo H, Rehncrona S, Soderfelt B, Olsson Y, Siesjö BK (1981) Brain lactic acidosis and ischemic cell damage: 2. Histopathology. J Cereb Blood Flow Metab 1:313–327

Kraig RP, Petito CK, Plum F, Pulsinelli WA (1987) Hydrogen ions kill brain at concentrations reached in ischemia. J Cereb Blood Flow Metab 7:379–386

Kumar K, Krause G, Koestner A, Hoehner T, White B (1987) Effect of flunarizine on global brain ischemia in the dog: a quantitative morphologic assessment. Exp Neurol 97:115–127

Lin CS, Polsky K, Nadler JV, Crain BJ (1990) Selective neocortical and thalamic cell death in the gerbil after transient ischemia. Neuroscience 35:289–299

Maršala J, Šulla I, Šanta M, Maršala M, Mechirova E, Jalč P (1989) Early neurohistopathological changes of canine lumbosacral spinal cord segments in ischemia-reperfusion-induced paraplegia. Neurosci Lett 106:83–88

Nauta WGH (1957) Silver impregnation of degenerating axons. In: Windle WF (ed) New research techniques of neuroanatomy. Thomas, Springfield, pp 17–26

Nedergaard M (1988) Mechanisms of brain damage in focal cerebral ischemia. Acta Neurol Scand 77:81–101

Nishikawa Y, Takahashi T, Shimoda A (1989) Morphological studies on cerebral cortical lesions induced by transient ischemia in mongolian gerbil – diffuse and peripheral pallor of the neuronal perikarya. Acta Neuropathol (Berl) 78:1–8

Paschen W, Schmidt-Kastner R, Djuricic B, Meese C, Linn F, Hossmann KA (1987) Polyamine changes in reversible cerebral ischemia. J Neurochem 49:35–37

Paschen W, Bengtsson F, Rohn G, Bonnekoh P, Siesjö B, Hossmann KA (1991) Cerebral polyamine metabolism in reversible hypoglycemia of rat: relationship to energy metabolites and calcium. J Neurochem 57:204–215

Pulsinelli WA, Brierley JB, Plum F (1982) Temporal profile of neuronal damage in a model of transient forebrain ischemia. Ann Neurol 11:491–498

Seubert P, Lee K, Lynch G (1989) Ischemia triggers NMDA receptor-linked cytoskeletal proteolysis in hippocampus. Brain Res 492:366–370

Sharp FR, Lowenstein D, Simon R, Hisanaga K (1991) Heat shock protein hsp72 induction in cortical and striatal astrocytes and neurons following infarction. J Cereb Blood Flow Metab 11:621–627

Siesjö BK (1988) Mechanisms of ischemic brain damage. Crit Care Med 16:954–963

Sloviter RS (1991) Permanently altered hippocampal structure, excitability, and inhibition after experimental status epilepticus in the rat: the "dormant basket cell" hypothesis and its possible relevance to temporal lobe epilepsy. Hippocampus 1:41–66

Smith ML, Auer RN, Siesjö BK (1984) The density and distribution of ischemic brain injury in the rat following 2–10 min of forebrain ischemia. Acta Neuropathol (Berl) 64:319–332

Switzer RC (1976) Neuronal argyrophilia induced by puromycin. A directed Golgi-like method. Neurosci Lett 2:301–305

Van den Pol AN, Gallyas F (1990) Trauma-induced Golgi-like staining of neurons: A new approach to neuronal organization and response to injury. J Comp Neurol 296:654–673

Yanagihara T, Brengman JM, Mushynski WE (1990) Differential vulnerability of microtubule components in cerebral ischemia. Acta Neuropathol 80:499–505